PHYSICAL REVIEW B VOLUME 25, NUMBER 2 15 JANUARY 1982

Bloch electrons in finite crystals in the presence of a uniform electric field

C. L. Roy and P. K. Mahapatra
Department of Physics, Indian Institute of Technology, Kharagpur 721302, India
(Received 2 April 1981)

Taking the crystal potentials to be of the Mathieu type, we have investigated the energy spectrum and the wave functions of Bloch electrons in finite crystals in the presence of a uniform electric field. Our main purpose is to examine the various aspects related to the (Wannier) Stark ladders (SL) in finite crystals. The treatment depends on solving the Schrödinger equation numerically; Gelarkin's approach, in combination with Householder's tridiagonalization procedure and the *Q-L* algorithm, is used for the purpose. Our investigation takes into account both the infinite-wall boundary conditions and the periodic boundary conditions, and it encompasses a wide range of parameters such as the crystal potential strength, the electric field, and the length of the crystal. The results obtained by us clarify the circumstances which would control the occurrence of SL and throw considerable light on the nature of the wave functions corresponding to the SL states.

I. INTRODUCTION

The study of the dynamics of Bloch electrons in the presence of a uniform electric field began long ago with the well-known Bloch's acceleration theorem.[1] In subsequent years, three developments added considerably to the interest in the subject. They are (a) the work of Zener[2] in connection with electrical breakdown in solid dielectrics, (b) the development of Houston's wave function,[3] and (c) the prediction of Stark ladders (SL) in crystals by Wannier.[4] Of these three aspects, which are interrelated, that of Stark ladders still seems to remain a topic of intensive theoretical as well as experimental studies. To see what features of Stark ladders still require serious consideration, it is necessary to review critically the salient works relevant to this phenomenon as a whole.

A Stark ladder, known currently as a Wannier Stark ladder, is essentially an equally spaced ladderlike splitting of the band levels of Bloch electrons, due to the presence of a uniform electric field. Wannier's prediction[4(a)] of this phenomenon is concerned with infinite crystals and is based substantially on the translational symmetry of the crystals. Briefly, Wannier's proof is as follows. The Schrödinger equation for an electron in a one-dimensional crystal in the presence of a uniform electric field E can be written as

$$H\Psi(x)=\epsilon\Psi(x), \tag{1.1}$$

where

$$H=-\frac{\hbar^2}{2m}\frac{d^2}{dx^2}+V(x)+eEx$$

and ϵ is the energy eigenvalue of the electron. The periodic crystal potential $V(x)=V(x-va)$, v being an integer and a the lattice spacing. When we let $x\rightarrow x-va$, Eq. (1.1) takes the form

$$H\Psi(x-va)=\epsilon_v\Psi(x-va), \tag{1.2}$$

where

$$\epsilon_v=\epsilon+veEa.$$

Considering (1.1) and (1.2) together, one can say that if $\Psi(x)$ is an eigenfunction of H with the eigenvalue ϵ, then $\Psi(x-va)$ is also an eigenfunction of H with the eigenvalue ϵ_v. The spectrum of energy levels ϵ_v constitutes a ladder, the separation between two consecutive levels in the ladder being eEa. This ladder of energy levels was called a Stark ladder by Wannier. According to a later analysis by Wannier,[4(b),4(c)] only one Stark ladder for each band should occur.

Wannier's prediction of the Stark ladder was critically examined by several authors from theoretical as well as experimental standpoints. While experimental work was concerned as expected with finite systems, theoretical studies were carried out for both infinite and finite systems. We first review the significant approaches followed in the theoretical study of the SL in infinite systems; this review is of great help in formulating the methods for probing the SL in finite systems—a topic to which this paper, as discussed later, is de-

voted.

The theoretical studies in regard to the SL in infinite systems were based on various approximations and mathematical techniques. Zak,[5] who used the k-q representation among other things, challenged the existence of Stark ladders. A point of Zak's criticism of Wannier's prediction is the argument that there is no restriction on ϵ [in (1.1) and (1.2)] that one starts with, and hence there is no reason to conclude that the energy spectrum is quantized; all energies, according to Zak, are allowed. Moyer[6] predicted that below a certain critical field, each energy band splits into not just one[4(b),4(c)] but many ladders, the number of such ladders increasing with a decrease in the electric field. Avron[7] pointed out that SL states are metastable. The works of Moyer and Avron aggravated the controversy initiated earlier by Zak about the validity of Wannier's prediction. Davison and coworkers[8–10] studied the problem of Stark ladders in infinite systems by using the tight-binding approximation (TBA), and their results indicated the occurrence of Stark ladders; however, later Avron *et al.*[11] pointed out certain limitations of the results obtained on the basis of the TBA. Lukes and Somaratna used[12] the Green's-function technique to study Stark ladders in infinite systems, and the present authors (Roy and Mahapatra) employed[13] the evolution operator techniqe in this regard; these works clarified several general aspects in relation to Stark ladders in infinite systems. It can be said at present that Stark ladders exist in infinite systems for fields which are not too high. The energy spectrum relevant to such Stark ladders is given[4(b),4(c),13(b),13(c)] as follows (the overbar indicates the average with k):

$$\epsilon_{n\nu}=\overline{\epsilon_n(k)}+\overline{eEX_{nn}(k)}+\nu\phi, \quad \nu=0,1,2,\ldots \tag{1.3}$$

where $\epsilon_{n\nu}$ is the energy of the νth level in the nth band,

$$X_{nn}(k)=\left\langle U_{n,k}\left|\frac{\partial}{\partial k_x}\right|U_{n,k}\right\rangle,$$

[$U_{n,k}$ is the periodic part of the Bloch function corresponding to nk, and $\phi = eEa$. The entity $eEX_{nn}(k)$ is the intraband shift of the levels $\epsilon_n(k)$ due to the presence of the electric field, while ϕ is the separation between two consecutive levels in the Stark ladder. The form of ϕ is the same as was predicted first by Wannier [Eq. (1.2)], and it will be referred to as Wannier spacing (WS). For very high fields, Zener tunneling becomes appreciable, giving rise to a broadening[13(b),13(c)] of the levels given by (1.3) and resulting thereby ultimately in a continuous energy spectrum. Obviously, therefore, one would not expect the occurrence of Stark ladders when the electric field is very high.

The above discussion gives a review of the major approaches and important findings regarding Stark ladders in infinite systems. Now, the systems we deal with in practice are finite and the results relevant to the infinite systems may not, for various reasons (discussed in the next paragraph), hold true for finite systems. Hence the question of Stark ladders in finite systems needs to be examined on its own footing. Before taking up the discussion of theoretical work on finite systems, we review the experimental investigation in regard to Stark ladders. The experimental results obviously provide a basis for judging the validity of the theoretical findings about Stark ladders in finite systems. The work of Koss and Lambert[14] is a significant experimental investigation of Stark ladders. The impetus to their experiment was supplied by an earlier theoretical work of Callaway,[15] who predicted that the absorption coefficient in the presence of a uniform electric field would possess a staircaselike structure if one assumes the existence of SL. Koss and Lambert measured the optical absorption coefficient in GaAs crystals in the presence of a uniform electric field and observed that Callaway's prediction is true. The results of Koss and Lambert can thus be taken as experimental evidence of the occurrence[13(c)] of Stark ladders. Another experiment that indicates the occurrence of Stark ladders was reported by Maekawa.[16] His investigation was concerned with the study of the variation of the conductivity with the electric field. Maekawa's results indicated oscillations of the conductivity with the electric field. The peaks of such oscillations were found to occur at the electric fields E given by $E=\hbar\omega/nae$, where ω is the long-wavelength phonon frequency. Maekawa's results were explained by Saitoh[17] on the assumption that Stark ladders exist.

As mentioned earlier, proper interpretation of the questions related to Stark ladders in practical systems is possible only by the theoretical treatment of the cases of finite systems in this respect. The mathematical approaches relevant to infinite systems are often not applicable to the finite cases; the difficulty arises out of the fact that the $\vec{k}$ values for the latter systems are discrete. A large number of studies of finite systems is carried out (I)

with an analysis of difference equations[18–21] obtained on the basis of the TBA, and (II) with the numerical solution[22–25] of the Schrödinger equation relevant to the problem. The treatment based on the TBA indicates, in a limited way, the occurrence of Stark ladders in finite systems. The approach of the TBA in regard to Stark ladders has, however, been criticized by some authors.[11,22] Compared with the approach of the TBA, the numerical solution of the Schrödinger equation with the use of suitable boundary conditions (BC) is expected to be a better method. (Recently, the numerical approach has been applied as well to infinite systems.[26]) Rabinovitch and Zak[24] (RZ) used the infinite-wall boundary conditions (IWBC) to study numerically the problem of Stark ladders in finite systems. They studied the energy spectrum as well as the wave functions for the purpose. Their energy spectrum did not reveal the occurrence of SL, and their wave functions did not correspondingly exhibit the localization expected of the SL states.[20] Later, Rabinovitch,[25] also using the IWBC, found that SL occur in finite systems only for very large periodic potentials. However, Rabinovitch did not study the wave functions, which are very essential for understanding several features of the SL.

From the discussion in the preceding paragraph, it appears that the understanding of the problem of SL in finite systems is not yet complete. The purpose of this paper is to make an exhaustive analysis of the various aspects related to the SL in finite systems. Our investigation is based on a numerical treatment of the Schrödinger equation, with the use of both the IWBC (Sec. II) and the periodic boundary conditions (PBC) (Sec. III). We have computed the energy spectrum as well as the wave functions, corresponding to a wide range of the periodic potentials and the electric field. The PBC are the only kind of boundary conditions which conform to the translational symmetry of the crystals[27] and are therefore considered to be more realistic than the IWBC. In view of the superiority of the PBC over the IWBC, we have put more emphasis on the former, and while the energy spectrum is computed for both kinds of the boundary conditions, the wave functions are obtained only for the PBC. The numerical approach (Sec. IV) we have followed is based on the use of Gelarkin's method,[28] together with Householder's tridiagonalization (HTD) procedure[29] and the Q-L algorithm.[29] Our results adequately clarify (Secs. V and VI) the circumstances that would control the occurrence of the SL in finite systems and throw considerable light on the nature of the wave functions associated with the SL states in such systems. In particular, our investigation leads to certain new criteria [Eqs. (5.2), (5.3), and (5.10)] governing the occurrence of SL in finite systems, and some of these criteria [(5.2) and (5.3)] explain convincingly (Sec. VI) why some earlier authors could not obtain any SL in finite systems. Furthermore, our work reports for the first time the transitional symmetry of the wave functions associated with Stark ladders in finite systems, and our results with the PBC are of special significance in the context of an analytical observation by Rabinovitch[27] regarding the compatibility of the PBC with finite crystals in the presence of an electric field.

II. THE TREATMENT WITH THE IWBC

We consider a one-dimensional Mathieu-type crystal in a constant electric field. Slater[30] discussed that the Mathieu-type crystal corresponds fairly well to realistic situations, and some authors studied[24,25] the one-dimensional Mathieu-type crystal also in regard to the SL. The situations just mentioned have prompted us to choose the Mathieu-type potential for describing the crystal potential. Now, the Schrödinger equation for our system appears as

$$H\Psi(x)=\epsilon\Psi(x), \tag{2.1}$$

where

$$H=-\frac{\hbar^2}{2m}\frac{d^2}{dx^2}+V(x)+eEx$$

and the Mathieu-type potential is

$$V(x)=2W\left[1-\cos\frac{2\pi x}{a}\right].$$

The crystal is considered to be of length $L\,(=Na)$ and the finiteness of the crystal is incorporated in the IWBC as follows:

$$\Psi(0)=\Psi(L)=0. \tag{2.2}$$

Taking the BC (2.2) into account, we solve the equation of motion (2.1) by using a method of Gelarkin.[28] The starting point for this method is the choice of the trial functions satisfying the prescribed boundary conditions. We choose, as our trial functions, the trigonometric function $\sin(i\pi x/L)$ $(i=1,2,\ldots)$. These functions obviously satisfy the BC (2.2). In terms of these trial functions, the approximate wave function Ψ_A is written as

$$\Psi_A(x)=\sum_{i=1}^{M} b_i \sin\left[\frac{i\pi x}{L}\right]. \tag{2.3}$$

If Ψ_A is to be the solution of (2.1), it should satisfy the following equation:

$$\int_0^L \left[\frac{\partial \Psi_A}{\partial b_i}(H-\epsilon)\Psi_A(x)\right]dx=0, \quad i=1,2,\ldots,M. \tag{2.4}$$

In view of (2.3), the set of M equations (2.4) leads to an eigenvalue equation of the form

$$\underline{B}\vec{b}=\epsilon\vec{b}. \tag{2.5}$$

$\vec{b}$ is a column vector with elements b_i. $\underline{B}$ is an $(M\times M)$ matrix which is real and symmetric; the elements of $\underline{B}$ are given by

$$B_{ij}=\left[\frac{h^2}{8mL^2}j^2+\frac{eEL}{2}+2W+W\delta_{Nj}\right]\delta_{ij}+\frac{4eELij}{(i^2-j^2)^2}[(-1)^{i+j}-1]\delta_{|i-j|r}-W\delta_{2N|i-j|}+W\delta_{2N(i+j)}\delta_{|i-j|r},$$
$$r=1,2,\ldots,M-1. \tag{2.6}$$

Equation (2.5) gives us the eigenvalue as well as coefficients b_i; by restoring the b_i's in (2.3), we get the wave functions. The numerical analysis pertinent to the computation of the energy spectrum and the wave functions in the light of (2.5) is discussed in Sec. IV.

III. THE TREATMENT WITH THE PBC

We consider here a finite Mathieu-type crystal subject to the PBC. The PBC, as mentioned in the Introduction, are more physical than the IWBC. The PBC can be expressed as

$$\Psi(x)=\Psi(x+L). \tag{3.1}$$

The behavior of the electrons is now described by the Schrödinger equation of motion (2.1) together with the BC (3.1). As we did in the case of the IWBC, we use the Gelarkin method[28] to solve also the Schrödinger equation under the PBC. For the present case, we choose as trial functions the trigonometric functions $\sin(2\pi ix/L)$ and $\cos(2\pi ix/L)$, which obviously satisfy the BC (3.1). The approximate wave function Ψ_A, in terms of these trial functions, can be written as

$$\Psi_A(x)=\frac{d_0}{\sqrt{2}}+\sum_{i=1}^{M}\left[d_{2i-1}\sin\left[\frac{2\pi ix}{L}\right]+d_{2i}\cos\left[\frac{2\pi ix}{L}\right]\right]. \tag{3.2}$$

If Ψ_A given by (3.2) is a solution of (2.1), it should satisfy (2.4) for every d_i; we would get in all $2M+1$ equations (the number of d_i's is $2M+1$) of type (2.4). In the light of (3.2), these $2M+1$ equations lead to the following eigenvalue equation:

$$\underline{D}\vec{d}=\epsilon\vec{d}. \tag{3.3}$$

$\vec{d}$ is a column vector with $2M+1$ d_i coefficients, while $\underline{D}$ is a real and symmetric matrix of order $2M+1$; the elements D_{ij} of $\underline{D}$ are given as follows:

$$\begin{aligned}D_{ij}=&\left\{\left[\frac{h^2}{2m}\left[\frac{s}{L}\right]^2+(-1)^{i+1}W\delta_{(N/2)s}\right](\delta_{[(i+1)/2]s}+\delta_{(i/2)s})+2W+\frac{eEL}{2}\right\}\delta_{ij}\\
&-\left[\frac{eEL}{\sqrt{2}\pi s}\right](\delta_{[(i+1)/2]s}\delta_{j0}+\delta_{i0}\delta_{[(j+1)/2]s})-\sqrt{2}W(\delta_{(i/2)N}\delta_{j0}+\delta_{i0}\delta_{(j/2)N})\\
&-\left[\frac{eEL}{4\pi s}\right](\delta_{[(i+1)/2]s}\delta_{(j/2)s}+\delta_{(i/2)s}\delta_{[(j+1)/2]s})+\frac{eELs}{\pi(r^2-s^2)}(\delta_{(i/2)r}\delta_{[(j+1)/2]s}+\delta_{[(i+1)/2]s}\delta_{(j/2)r})\delta_{|s-r|q}\\
&-W[\delta_{N|r-s|}+(-1)^i\delta_{N(r+s)}\delta_{|s-r|q}](\delta_{[(i+1)/2]s}\delta_{[(j+1)/2]r}+\delta_{(i/2)s}\delta_{(j/2)r}),\end{aligned} \tag{3.4}$$

where

$$i,j=0,1,\ldots,2M,$$

$$q,r,s=1,2,\ldots,M.$$

Equation (3.3) determines the energy eigenvalues (ϵ) and the coefficients d_i, which later give us the wave functions via (3.2). The numerical analyses pertinent to the use of (3.3) for computing the energy spectrum and the wave functions are discussed in the next section.

IV. NUMERICAL ANALYSES

We have carried out numerical analyses concerning the energy spectrum and the wave functions, as well as some other features related to them. The energy spectrum has been computed for both the IWBC and PBC, while the wave functions are computed only for the PBC. The procedure for computing the energy spectrum is to solve the equations relevant to the determinantal compatibilities of the matrix equations (2.5) and (3.3), corresponding, respectively, to the IWBC and PBC; the matrices $\underline{B}$ and $\underline{D}$ are of orders 100 and 105, respectively. For the purpose of computing the wave functions (corresponding to the PBC only), the eigenvector $\vec{d}$ is also evaluated and used in (3.2).

The numerical technique used throughout is the Householder's tridiagonalization (HTD) method, in combination with the Q-L algorithm.[29] This particular numerical procedure is followed for the reason that an approach of this sort alone can give us the complete set of the wave functions and energy eigenvalues. We have discussed in the Appendix the mathematical features of the method and also indicated its merit and degree of accuracy.

The energy spectrum is given in Figs. 1—4, and the wave functions are shown in Figs. 5—7. Using the results relevant to Figs. 1—4, we have computed the values of certain entities such as the maximum level separation in the absence of the electric field ($E=0$) and the Wannier spacing ϕ ($\phi=eEa$). These results are shown in Tables I and II; as discussed later, they are of great help (Sec. V) in establishing certain criteria regarding the occurrence of Stark ladders. Further, we have studied the localization length relevant to the wave functions. The localization length ξ_l is defined as

$$\xi_l=\xi_1+\xi_2. \tag{4.1}$$

ξ_1 and ξ_2 satisfy the following equations:

$$\frac{|\Psi(x_0+\xi_1)|^2}{|\Psi(x_0)|^2}=\exp(-1), \tag{4.2}$$

$$\frac{|\Psi(x_0-\xi_2)|^2}{|\Psi(x_0)|^2}=\exp(-1), \tag{4.3}$$

where x_0 is the point at which $|\Psi|^2$ has the peak value. Using the graphs of Figs. 5—7, we computed the localization length as a function of certain pertinent parameters and show these results in the Figs. 8 and 9. These results help us to obtain a substantial grasp of the relation between the occurrence of the SL and the localization of the SL states.

V. RESULTS

A. Energy spectrum for the IWBC

As discussed in Sec. IV, the energy spectrum corresponding to the IWBC is computed on the basis of (2.5); the results in this respect are shown in the graphs of Figs. 1 and 2. The energy spectrum is computed for varying values of the length L, the crystal potential strength W, and the electric field E; these three parameters are closely related to the problem.

The graphs in Fig. 1 show the general pattern of the energy spectrum for different fields for $W=4.5$ eV. The energy eigenvalues for the zero-field case show the usual features. Thus, they have direct connection with the wave number k, and group themselves into allowed bands separated by forbidden gaps, except for one allowed energy value which falls in a forbidden gap and corresponds to a surface state. Furthermore, the number of levels in an allowed band equals the number (20 in our case) of unit cells in the crystal. With the application of the field, the energy eigenvalues become a function of the number monitoring the states, and we notice the occurrence of Stark ladders in certain cases. Thus for $E=3\times10^8$ V/m, the smaller of the two fields in Fig. 1, all energy eigenvalues of the first band except the two levels near the band edges form a Stark ladder, i.e., they are equally spaced. The spacing between the levels forming the SL is seen to be 0.1696 eV, which corresponds to the Wannier spacing ϕ as given in (1.3), and the spacing between the two levels near the band edges differs from the level spacing in the SL by about 2%. With regard to the case of the second band

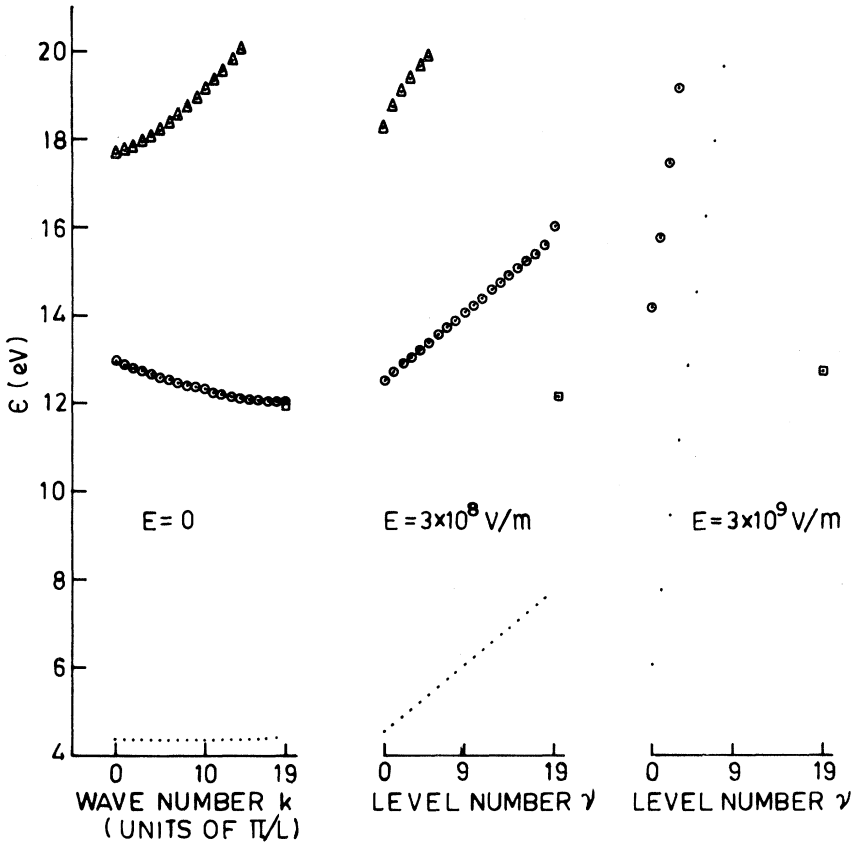

FIG. 1. Energy spectra for a finite Mathieu-type crystal in the presence of uniform electric fields E and subjected to IWBC. The crystal parameters are as follows: $W=4.5$ eV, $L=20a$, and $a=5.6532$ Å. In the absence of the field ($E=0$), the dependence of the energy levels (ϵ) on the wave number (k) is shown. In the presence of the field ($E=3\times10^8$ and 3×10^9 V/m), the dependence of the energy levels (ϵ) on the level number (ν) is shown. For all the three values of E, the identification of the energy levels is as follows: •, levels of the first band; ⊙, levels of the second band; ◬, levels of the third band; ⊡, surface levels.

for this field, about 11 levels near the center out of a total of 20 levels form a Stark ladder, while no Stark ladder occurs in a band higher than the second one. The occurrence of a Stark ladder for a fraction of the levels in the second band corroborates the idea of quasi-Stark-ladders reported by Heinrich and Jones.[18] Considering those graphs in Fig. 1 which correspond to the higher field (3×10^9 V/m), we find that SL occur now in both the first and second band, but not in any other higher band. The SL spacing is seen to be 1.6959 eV, which again corresponds to the WS ϕ. It is noteworthy that the SL in the two bands have an overlap. We find that in the cases where complete SL exist (i.e., the first band levels for $E=3\times10^8$ V/m and the first and second band levels for $E=3\times10^9$ V/m), the zeroth level, ϵ_{n0}, corresponds to (1.3):

$$\epsilon_{n0}=\overline{\epsilon_n(k)}+eE\overline{X_{nn}(k)}. \tag{5.1}$$

The results in the graphs of Fig. 2 illustrate the effect of the variation of the crystal length on the SL pattern; also, comparison of the results in Figs. 1 and 2 would indicate the effect of the change of the crystal potential on the SL. The values chosen for a (=5.6532 Å) and W (=0.75 eV) are similar to those in GaAs crystal—a system used in experimental studies[14] of SL. It is seen that for the particular field (i.e., 8.495×10^7 V/m) chosen, SL do not occur for $L=20a$, but they do occur for the higher length $L=50a$. To comprehend thoroughly the roles of the length of the crystal and the crystal potential on the occurrence of SL, we have compiled Table I by using, as mentioned earlier (Sec. IV), the results relevant to Figs. 1 and 2. This table, together with Figs. 1 and 2, indicates that the Stark ladder begins to occur at first around the center of the band if the following inequality is satisfied:

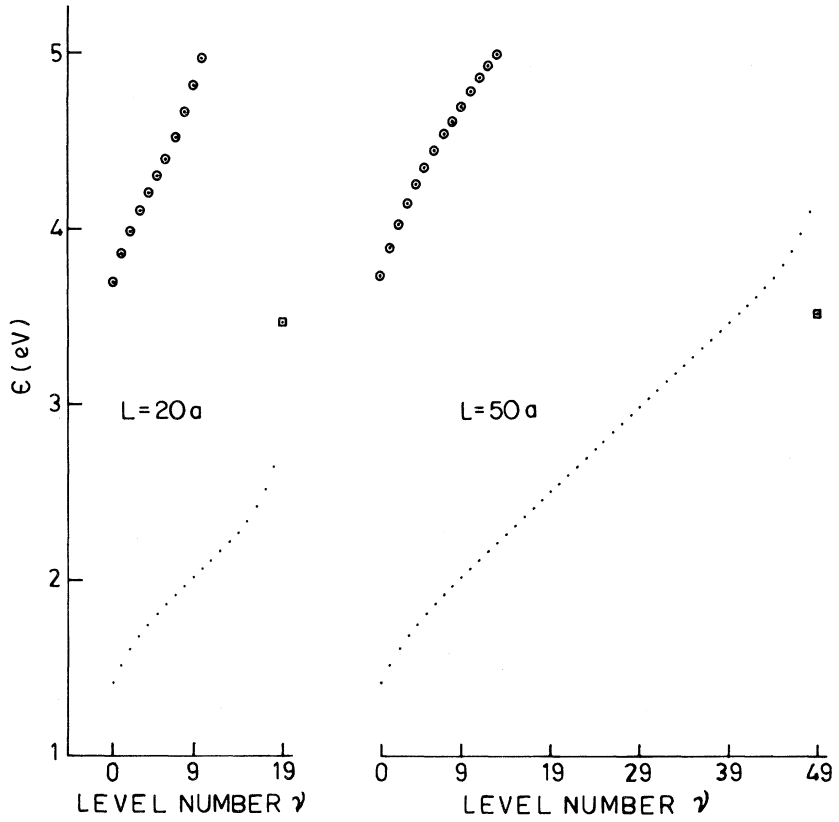

FIG. 2. Comparison of the energy spectra of two finite Mathieu-type crystals in a uniform electric field and subjected to IWBC. The crystals are of length $20a$ and $50a$. All other parameters are the same for both lengths; their values are as follows: $W=0.75$ eV, $E=8.495\times 10^8$ V/m, and $a=5.6532$ Å. The graphs show the dependence of the energy levels (ϵ) on the level number (ν): •, levels of first band; ⊙, levels of second band; ⊡, surface levels.

$$(\Delta_{\max})_{nI} < eEa \,, \tag{5.2}$$

where $(\Delta_{\max})_{nI}$ is the maximum level separation in the nth band for $E=0$ under the IWBC. The table further suggests that a larger number of levels get involved with the SL when inequality (5.2) becomes more pronounced. Now it is known that the maximum (zero-field) level separation in any band would be smaller for larger W and larger L. Hence, in view of (5.2), we expect that when the field and the crystal potential are fixed, the occurrence of SL would be favored if L is large. This explains the difference with respect to the results for $L=20a$ and $50a$ in Fig. 2. In view of (5.2), we note also that when the length and the field are given, the chance of occurence of the SL would become large if the electrons are very tightly bound.

B. Energy spectrum for the PBC

The energy spectrum corresponding to the PBC is shown in the graphs of Figs. 3 and 4. The value of W in Fig. 3 is quite high (4.5 eV); this choice makes the maximum value of the (zero-field) level separation small or, equivalently, the band gap large. These situations allow us to examine the SL over quite wide ranges of the electric field. The value of W in Fig. 4 is quite small (0.75 eV) and is similar to the crystal potential in GaAs, as was the case in Fig. 2; the results in Fig. 4 would help explain the occurrence of the SL for weakly bound electrons.

Considering Fig. 3, we find that for $E=0$ the states (as expected) group themselves into allowed bands separated by forbidden gaps, the number of states in any band equaling that of the unit cells (21) in the crystal. Furthermore, the states have direct connection with the wave number and they are doubly degenerate. With the application of the field, the distribution of the states changes, the energy eigenvalues in each band becoming (as they do for the case of IWBC) functions of the number monitoring the states. For $E=3\times 10^8$ V/m, the lower of the two fields, all the levels in the first

TABLE I. The entries in this table are relevant to the results in Figs. 1 and 2. The total number of levels in a band equals the number of unit cells. The symbol $(\Delta_{\max})_{nI}$ means the maximum level separation in the nth band for $E=0$ under the IWBC. Values with asterisks are approximate.

W (eV)	Number of unit cells	Band number (n)	$(\Delta_{\max})_{nI}$ (eV)	E (V/m)	ϕ (eV)	Number of levels forming SL	Remarks
4.5	20	1	0.009 32	3×10^{8}	0.1696	17	SL exist for almost all levels
4.5	20	2	0.069 47	3×10^{8}	0.1696	11	SL exist partly
4.5	20	1	0.009 32	3×10^{9}	1.6959	19	SL exist for all band levels
4.5	20	2	0.069 47	3×10^{9}	1.6959	19	SL exist for all band levels
0.75	20	1	0.048 03	1.6×10^{7}	0.009 04	0	SL do not occur
0.75	20	1	0.048 03	8.495×10^{7}	0.048 02	0	SL do not occur
0.75	40	1	0.025*	5.2×10^{7}	0.0294	12	SL exist partly
0.75	50	1	0.02*	8.495×10^{7}	0.048 02	24	SL exist partly
0.75	50	2	0.085*	8.495×10^{7}	0.048 02	0	SL do not occur

band, except the surface state, form SL. In the second band there occurs a partial SL involving all levels, except the surface state and three levels each near the top and bottom of the band. In regard to the third and still higher bands, no SL is seen to occur. For this field, the SL spacing (0.1696 eV) in both the first and the second bands again corresponds to the WS, ϕ. Compared to the cases of Fig. 1, a larger fraction of levels (all 20 levels in the first band and 14 out of 20 in the second band), is now involved with the SL. This difference is explainable in light of condition (5.3), taking into account the fact that the length of the crystal for the present situation is slightly larger than that corresponding to Fig. 1; condition (5.3) is similar to (5.2) and is described later in detail. For the higher field ($E=3\times10^{9}$ V/m) in Fig. 3, SL are observed in both the first and second bands except for the surface state in each of the two bands. The SL here, like those in Fig. 2, overlap and the level spacing in the SL corresponds to WS. For both fields in Fig. 3, the zeroth level corresponds to (5.1) when complete SL are present (i.e., the levels in the first band for $E=3\times10^{8}$ V/m and the levels in both the first and the second bands for $E=3\times10^{9}$ V/m).

The results in Fig. 4 are obtained for a system which is, as mentioned earlier, similar to a one-dimensional GaAs crystal. The graphs indicate the results for $E=0$, 7.5×10^{7}, 1.25×10^{8}, and 2.5×10^{8} V/m. We have also computed the energy eigenvalues for $E=5\times10^{9}$ V/m; these results are not given in the graphs but are discussed below. For $E=7.5\times10^{7}$ V/m, no SL occur. For $E=1.25\times10^{8}$ and 2.5×10^{8} V/m, SL occur partially only in the first band; out of a total of 20 band states, the number of levels involved with the SL for the two fields is, respectively, 8 and 13. For E

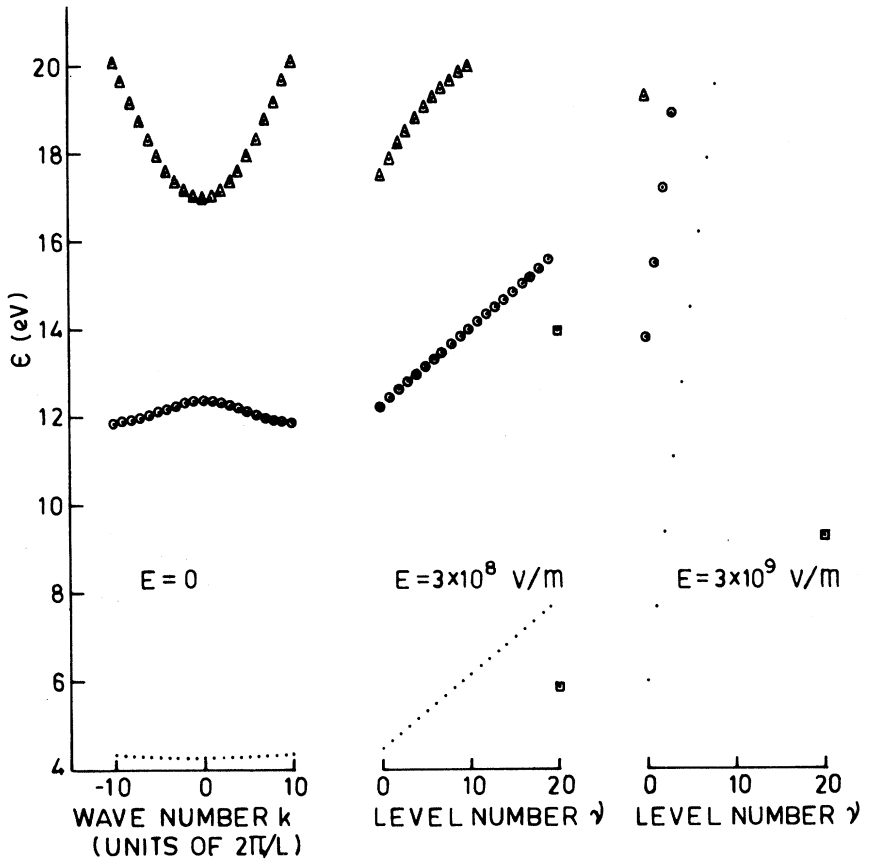

FIG. 3. Energy spectra for a finite Mathieu-type crystal in presence of uniform electric fields (E) and subjected to PBC. The crystal parameters are as follows: $W=4.5$ eV, $L=21a$, and $a=5.6532$ Å. In the absence of the field ($E=0$), the dependence of the energy levels (ϵ) on the wave number (k) is shown. In presence of the field ($E=3\times10^8$ and 3×10^9 V/m) the dependence of the energy levels on the level number (ν) is shown: •, levels of the first band; ⊙, levels of the second band; ▲, levels of the third band; ⊡, surface levels.

$=5\times10^9$ V/m, we observe no kind of SL in any band. This field is very high and is likely to give rise to an appreciable Zener tunneling. The occurrence of Zener tunneling is expected to be responsible for the absence of the SL in a finite system under very high fields, in very much the same way as it disturbs the SL in infinite systems.[13(b),13(c),26] For thorough comprehension of the observations relevant to Figs. 3 and 4, we have compiled Table II. The conclusions one can draw from Table II are similar to those relevant to the inequality (5.2), the inequality for the present case being, of course, given by

$$\tfrac{1}{2}(\Delta_{\max})_{nP} < eEa \,. \tag{5.3}$$

$(\Delta_{\max})_{nP}$ is the maximum level separation in the nth band for $E=0$ under the PBC. The factor $\frac{1}{2}$ in (5.3) is due to the second-order degeneracy of the levels under the PBC.

C. The wave functions and the related aspects

The wave functions, computed for only the PBC, are shown in Figs. 5–7. Figure 5 shows the results for $E=0$, and the others indicate the wave functions in the presence of electric fields. We take first the cases for $E=0$. RZ pointed[24] out that, in the absence of an electric field, the wave functions near the nondegenerate band edges can be interpreted in terms of the effective-mass approximation (EMA); according to the EMA, the wave functions can be described as a product of the Mathieu function and a sine (or cosine) function. Our results corroborate this observation of RZ with respect to

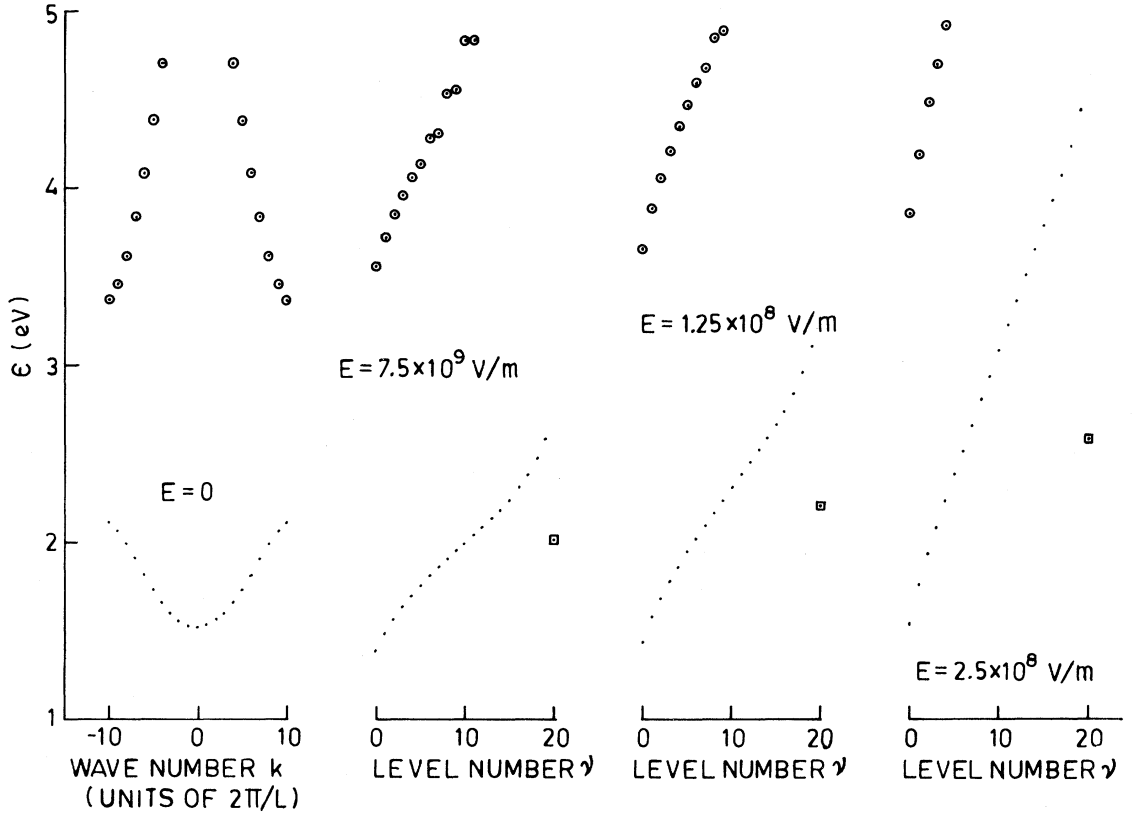

FIG. 4. Energy spectra for a finite Mathieu-type crystal in the presence of an electric field (E) and subjected to the PBC. The crystal parameters are as follows: $W=0.75$ eV, $L=21a$, and $a=5.6532$ Å. In the absence of a field ($E=0$), the dependence of the energy levels (ϵ) on the wave number (k) is shown. For $E\neq 0$ ($E=7.5\times 10^7$, 1.25×10^8, and 2.5×10^8 V/m), the dependence of the energy levels (ϵ) on the level number (ν) is shown: •, levels of the first band; ⊙, levels of the second band; ⊡, surface levels.

the wave functions near the nondegenerate band edges. However, we note that the zero-field wave functions near the degenerate band edges cannot be described in terms of the EMA. This finding emerges from the nature of the wave functions near the edges of the first and second bands in Figs. 5(a) and 5(b). Let us first look at the cases of the nondegenerate band edges. The lowest state in the first band ($\epsilon=4.274\,949$ eV) and the highest state in the second band ($\epsilon=12.393\,86$ eV) are nondegenerate, and some states around these two can be described in terms of the EMA. The mathematical forms Ψ_1 and Ψ_2 of the wave functions corresponding, respectively, to the states near the bottom of the first band and the top of the second band, appear as follows:

$$\Psi_1=ce_0(\omega)f\left[\frac{2q\omega}{N}\right], \tag{5.4}$$

$$\Psi_2=se_2(\omega)f\left[\frac{2q\omega}{N}\right], \tag{5.5}$$

where $ce_0(\omega)$ and $se_2(\omega)$ are the two Mathieu functions, $\omega=\pi x/a$, and $f(y)=\sin(y)$ or $\cos(y)$. q is an integer characterizing the states near the bottom of the band; in practice, q can take the values 0, 1, or 2. That the EMA fails for those band edges where the states are degenerate can be inferred by looking at the wave functions near the top of the first band ($\epsilon=4.320\,738$ eV) and the bottom of the second band ($\epsilon=11.896\,411$ eV). If the EMA were valid for the wave functions near the top of the first band, they would correspond to

$$se_1(\omega)\cos\left[2\left[\frac{N}{2}-\beta\right]\frac{\omega}{N}\right]$$

or

TABLE II. The entries in this table are relevant to the results in Figs. 3 and 4. The total number of levels in a band equals the number of unit cells. The symbol $(\Delta_{\max})_{nP}$ means the maximum level separation in the nth band for $E=0$, under the PBC.

W (eV)	Number of unit cells	Band number (n)	$\frac{1}{2}(\Delta_{\max})_{nP}$ (eV)	E (V/m)	ϕ (eV)	Number of levels forming SL	Remarks
4.5	21	1	0.003 08	3×10^{8}	0.1696	20	SL exist for all band levels
4.5	21	2	0.038 98	3×10^{8}	0.1696	14	SL exist partly
4.5	21	1	0.003 08	3×10^{9}	1.6959	20	SL exist for all band levels
4.5	21	2	0.038 98	3×10^{9}	1.6959	20	SL exist for all band levels
0.75	21	1	0.045 46	7.5×10^{7}	0.0424	0	SL do not occur
0.75	21	1	0.045 46	1.25×10^{8}	0.070 66	8	SL exist partly
0.75	21	1	0.045 46	2.5×10^{8}	0.141 33	13	SL exist partly
0.75	21	1	0.045 46	7.5×10^{8}	0.424	16	SL exist partly

$$_{s}e_1(\omega)\sin\left[2\left[\frac{N}{2}-\beta\right]\frac{\omega}{N}\right],$$

where β is an integer around $N/2$ but less than $N/2$. Similarly, if the EMA were valid near the bottom of the second band, the wave functions there would correspond to

$$_{c}e_1(\omega)\cos\left[2\left[\frac{N}{2}-\beta\right]\frac{\omega}{N}\right]$$

or

$$_{c}e_1(\omega)\sin\left[2\left[\frac{N}{2}-\beta\right]\frac{\omega}{N}\right].$$

The graphs relevant to these wave functions [Figs. 5(a) and 5(b)] indicate that they are much more complicated than what the EMA requires them to be.

We now analyze the wave functions in the presence of the electric field; these wave functions are shown in Figs. 6(a) and 6(b). We have taken $E=3\times10^{8}$ V/m and the crystal potential the same as that for Figs. 5(a) and 5(b). We first consider some aspects related to the localization of the wave functions, and we find it useful to recall in this context the results in Fig. 3, which provide the energy spectrum for the situations in Figs. 6(a) and 6(b). We note that the energy spectrum pertinent to the wave functions of Figs. 6(a) and 6(b) is such that all energy eigenvalues in the first band, except the surface state, form a complete SL, whereas in the second band, only some levels around the center of the band group themselves in the form of one SL. Figures 6(a) and 6(b) show that the wave function corresponding to the nth level becomes localized around the $(n+1)$th atom. The localization for a certain level in the first band is more than that for the corresponding level in the second band. This observation, in view of the aforementioned features of the energy spectrum in the first and second bands, suggests that the wave function is

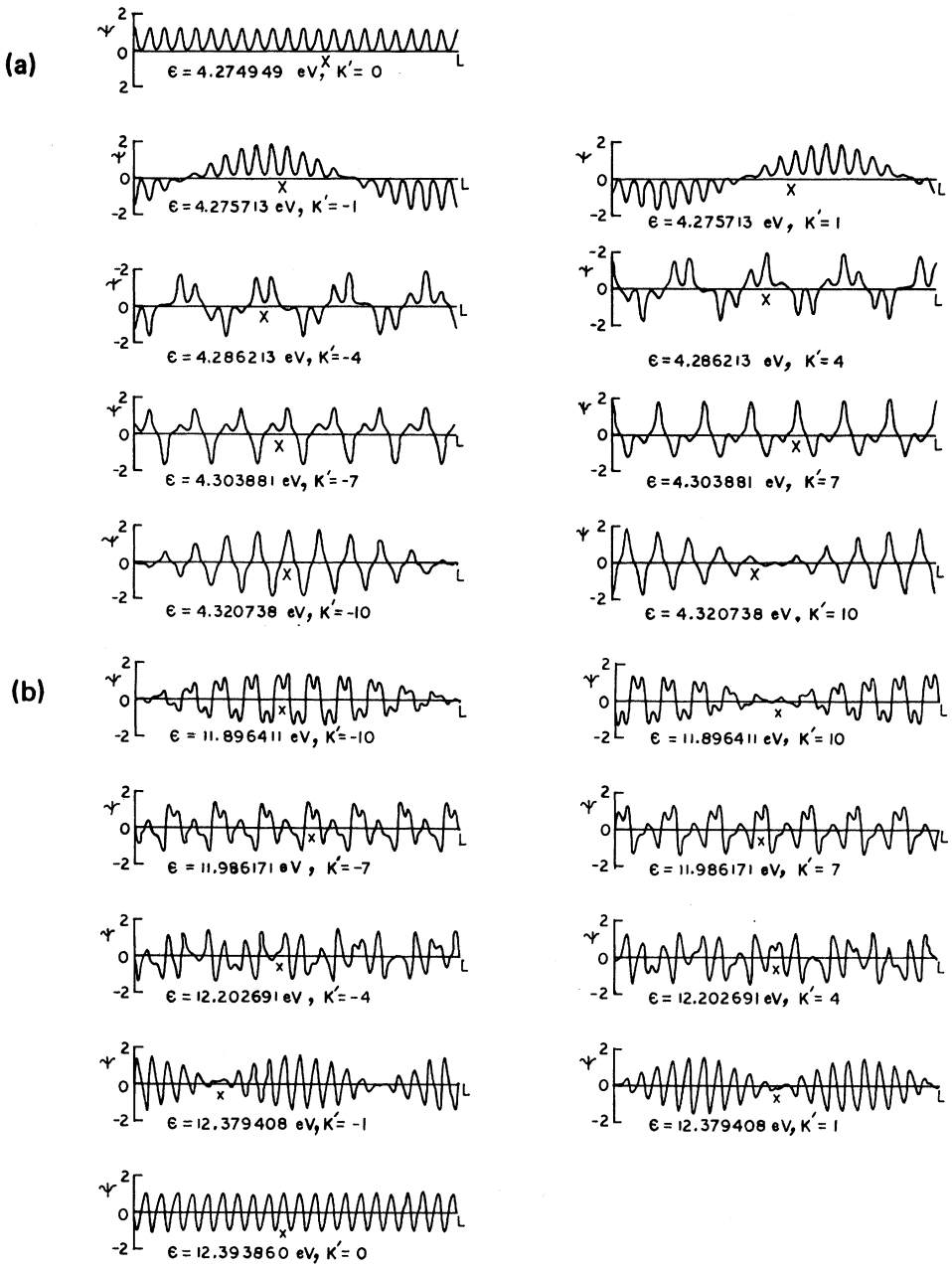

FIG. 5. (a) Wave functions for a finite Mathieu-type crystal in the absence of an electric field ($E=0$). The crystal parameters are $W=4.5$ eV, $L=21a$, and $a=5.6532$ Å. The entity K' is related to the wave number (k) as $K'=kL/2\pi$. All of these wave functions refer to the first band and correspond to the use of PBC. (b) Wave functions in the second band for a finite Mathieu-type crystal under the same conditions as those in (a).

most highly localized for the states in those bands where complete Stark ladders occur. Besides the SL states, the surface states also show localization near the end atoms in the chain. The surface states in Figs. 6(a) and 6(b) are those corresponding, respectively, to $\epsilon=5.836\,509$ and $13.945\,39$ eV.

That the wave functions for the SL states should be localized is one of the main characteristics[20] of such states, and our numerical treatment also corroborates this feature of the SL states. Further discussion of the localization of SL states is given later.

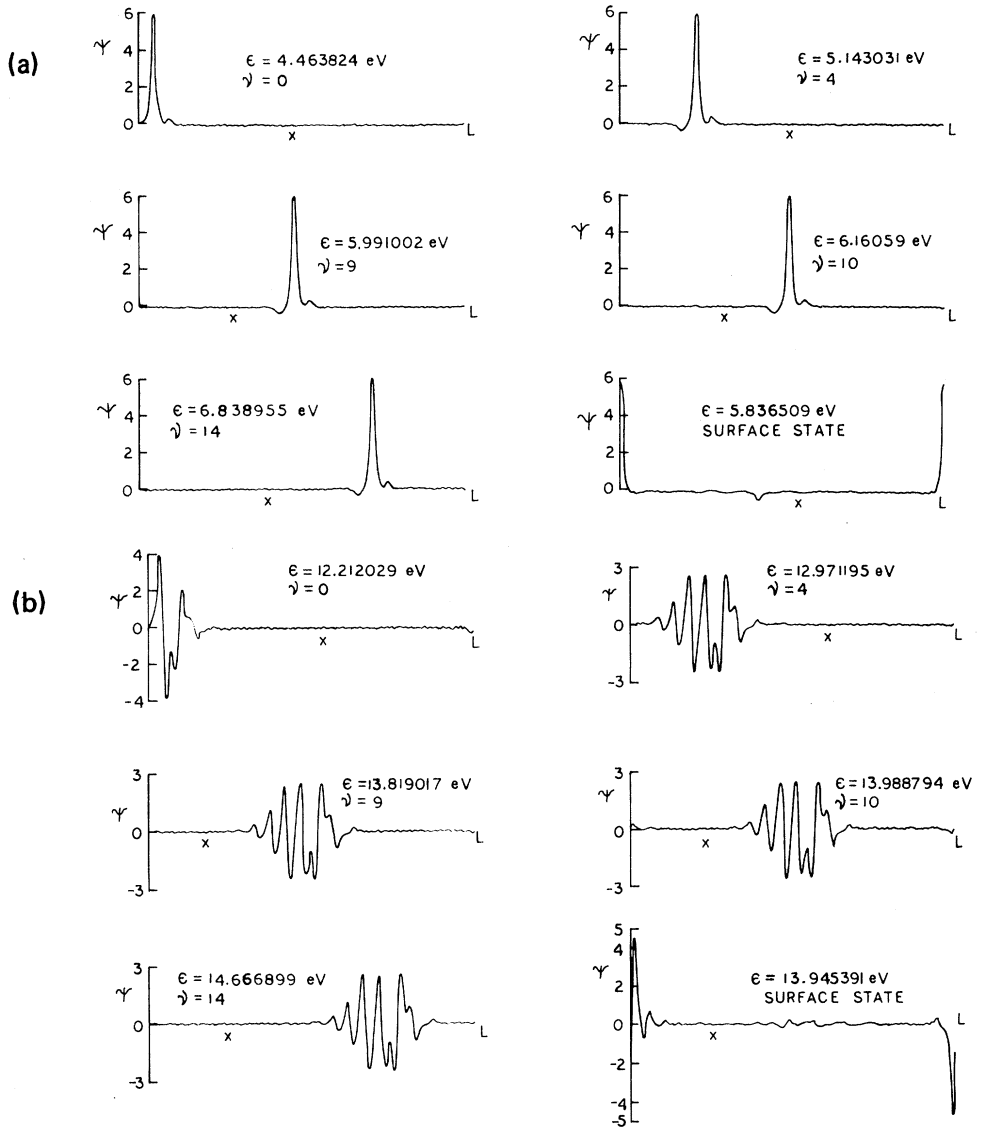

FIG. 6. (a) Wave functions of a finite Mathieu-type crystal in presence of an electric field, $E=3\times10^8$ V/m. The oth- parameters are $W=4.5$ eV, $L=21a$, and $a=5.6532$ Å. All of these wave functions refer to the first band and correspond to the PBC. (b) Wave functions in the second band for a finite Mathieu-type crystal in presence of an electric field, under the same conditions as those in (a).

The graphs in Figs. 6(a) and 6(b) establish that the wave functions of the SL states follow the translational symmetry[4(a),4(b)] as expressed by

$$\Psi_{n,\nu+\mu}(x+\mu a)=\Psi_{n,\nu}(x), \tag{5.6}$$

where $n=1$, 2 is the band index and ν and μ are positive integers such that $\nu+\mu<N$. The translational symmetry is absent for the states which do not form SL. An example of such states is provided by the wave function corresponding to $\epsilon=12.212029$ eV in Fig. 6(b); this state pertains to the lower edge of the second band for $E=3\times10^8$ V/m in Fig. 3.

The question as to whether the EMA is applicable to the wave functions in the presence of an electric field deserves serious considerations. According to the EMA, the wave functions for the electrons in a finite Mathieu-type crystal under a uniform electric field should be the product of a Mathieu function and a combination of the Airy functions Ai and Bi, this combination depending upon the BC one uses (PBC in our case). The wave

functins for the SL states shown in Figs. 6(a), 6(b), and 7 do not resemble any such product just mentioned, and hence the EMA does not seem to be applicable to the SL states. This observation of ours appears to contradict a prediction of RZ.[24] However, for the cases where SL do not occur [i.e., for small fields E where (5.3) is not satisfied], the wave functions (not shown in the figures) were found to resemble what RZ reported, and it may be possible to interpret such wave functions in terms of the EMA.

The nature of the wave functions of the SL states depends significantly on the bandwidth, ϵ_{bw}, and the SL spacing ϕ $(=eEa)$. The situation in this respect is displayed in Figs. 7 and 8. Figure 7 shows in a general way how the spread of the wave functions depends on ϵ_{bw} and E. More useful information is provided by Fig. 8 which shows the localization length (ξ_l) [introduced in (4.1)] as a function of the ratio ϵ_{bw}/ϕ. The graph in this figure leads to the following relation:

$$\xi_l=\xi_0+\rho\eta a\,, \tag{5.7}$$

where $\eta=\epsilon_{bw}/\phi$, $\rho\simeq 1$. ξ_0 can be interpreted as the localization length for the isolated atom and $\rho\eta$ is a measure of the additional spread of the wave function due to the combined action of the electric field and the crystal potential. To see definitely how the degree of localization of the wave functions is connected with the occurrence of SL, we have plotted the graph in Fig. 9; this graph leads to the following relation:

$$\xi_l=\xi_0'+(0.588)Za\,, \tag{5.8}$$

where

$$Z=\frac{N(\Delta_{\max})_P}{\phi}\,,$$

$$\xi_0'\simeq\xi_0=0.33a\,.$$

$(\Delta_{\max})_P$ is the maximum level separation according to the PBC for $E=0$. Combining (5.8) with (5.3), we come to the conclusion that for the occurrence of SL, the following inequality must be satisfied:

$$\xi_l<\xi_0'+0.588L\,. \tag{5.9}$$

Noting that $\xi_0'=0.33a$, (5.9) can be reduced to

$$\xi_l<\alpha L\,, \tag{5.10}$$

where $\alpha=0.33/N+0.588$.

VI. CRITICAL DISCUSSION AND CONCLUDING REMARKS

In Sec. V, we have indicated the various features of our results, more or less on their own merits. In this section, we discuss critically and pointedly how our findings compare with other results, relevant to both finite and infinite systems. We emphasize in this context the following aspects.

A. The energy spectrum and the occurrence of Stark ladders

Our study indicates that Stark ladders would occur in finite crystals, under both IWBC and PBC,

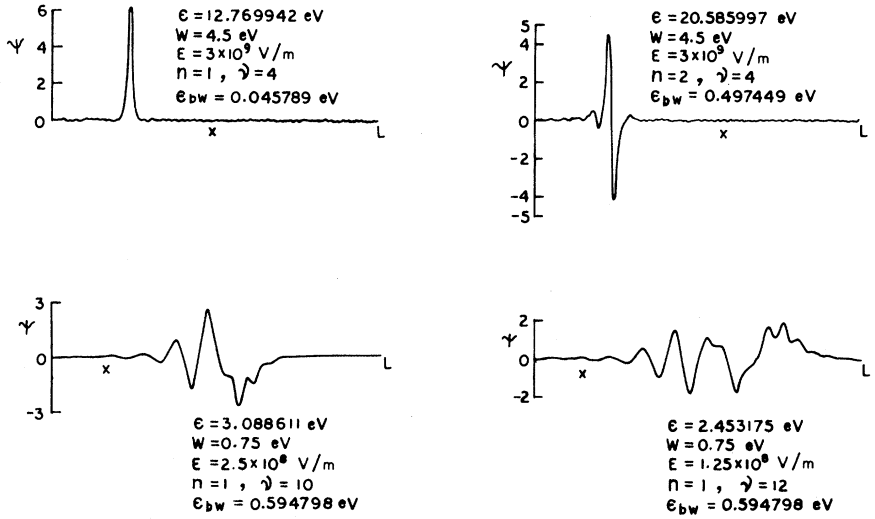

FIG. 7. Wave functions of a finite Mathieu-type crystal in the presence of uniform electric fields and subjected to PBC. The electric field (E) and various other parameters relevant to those wave functions are shown in the figure. The parameter ϵ_{bw} corresponds to the bandwidth for $E=0$. For all graphs, $L=21a$ and $a=5.6532$ Å.

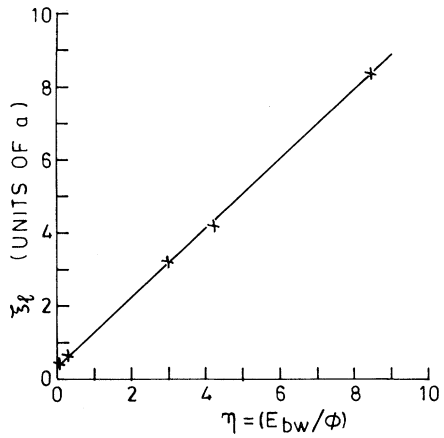

FIG. 8. Variation of localization length (ξ_l) of the wave functions of the SL states with ϵ_{bw}/ϕ; ϵ_{bw} is the zero-field bandwidth and ϕ ($=eEa$) is the Wannier spacing. The calculated values of ξ_l are indicated by $\times$.

provided certain criteria are satisfied. These criteria, called henceforth as existence conditions, are (5.2) and (5.3), corresponding, respectively, to the IWBC and PBC. The existence conditions give the lowest value of the field at which the levels around the center of the band start forming a (partial) Stark ladder, with more levels joining the Stark ladder as the inequality becomes more and more pronounced. Furthermore, the existence conditions reveal that, in general, the electric field, the periodic crystal potential, and the length of the crystal,

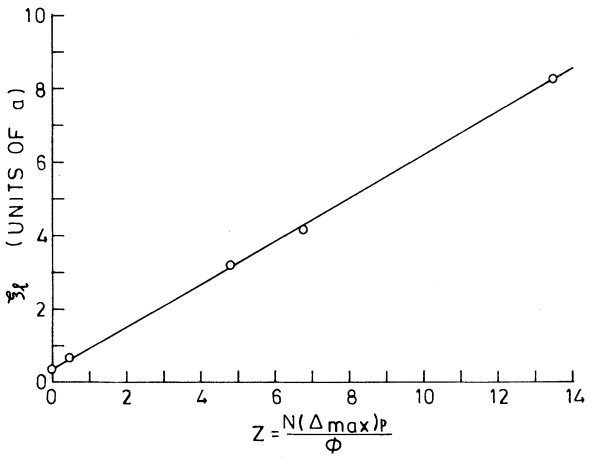

FIG. 9. Variation of the localization length (ξ_l) of SL states with some pertinent parameters; N is the number of units cells in the chain, $(\Delta_{max})_P$ is the maximum level separation (under the PBC) for $E=0$. The calculated values of ξ_l are indicated by $\circ$.

all have a role to play in connection with the occurrence of the SL. Now, three questions arise in regard to the just-mentioned features we obtained for the energy spectrum. They are the following: (a) How do the SL in finite systems compare with the SL in infinite system? (b) How does our finding that SL can occur in finite systems compare with other theoretical work in this respect? (c) How do our results compare with experimental findings, which are obviously pertinent to the finite system?

In regard to question (a), we find that when SL occur in finite systems they possess certain characteristics typical of the SL in infinite systems. Thus (I) the spacing in the SL in finite systems is the same as ϕ predicted[4(a)] by Wannier for infinite systems, this equality being true for both the complete and partial SL in finite systems, (II) for complete SL in finite systems, the zeroth level is located in the same way as predicted[4(b),4(c),13(b),13(c)] for the SL in infinite systems, and (III) the absence of SL in finite systems under high fields can be explained in terms of the occurrence of Zener tunneling in the same way as explained for infinite systems.[13(b),13(c),26]

In regard to question (b), we note first that our results generally confirm the findings of Sessa and Sitte[22] and Rabinovitch[25]; these authors carried out numerical studies to show that SL exist in finite systems under certain conditions. Moreover, the fact that we obtained partial SL in certain cases corroborates the idea of quasi-Stark ladders reported earlier by some authors.[18,21] Our results, however, are in disagreement with those obtained[24] by RZ. We find that this disagreement can be resolved amicably if we make use of inequality (5.2), together with the role of the Zener tunneling. The absence of SL in the work of RZ for the lower values of the field is due to the fact that these fields and the relevant parameters (Fig. 5 in Ref. 24) do not satisfy inequality (5.2); the reason why they did not obtain any SL for higher fields (Fig. 7 in Ref. 24) is due to the fact that these fields are very large and they give rise to appreciable Zener tunneling. The arguments just given also explain the absence of the SL in the empty lattice case treated by RZ (Fig. 2 in Ref. 24); for this system, the band gap is negligibly small and any field for which existence condition (5.2) is satisfied would give rise to an appreciable Zener tunneling, thus barring the occurrence of SL.

Coming to question (c), we recollect that a few experimental investigations[14,16] indicated the existance of SL; these positive experimental results ob-

viously confirm the occurrence of SL in finite systems. We can easily check that the circumstances under which the experiments on SL were carried out conform with our existence conditions and, moreover, they make the effect of the Zener tunneling insignificant. For instance, Maekawa[16] made use of the following parameters: the band gap, E_G ($\simeq 2W$)$=3$ eV, $N=3\times 10^3$, $E=10^8$ V/m. For these parameters, inequality (5.3) is easily satisfied, due mainly to the higher value of N. Furthermore, a band gap of 3 eV is too high to permit any appreciable Zener tunneling for the value of E used in the experiment.

We would now like to mention how our results appear in the context of a study done by Rabinovitch.[27] The fact that we have obtained solutions to (2.1) under the PBC is in contradiction to Rabinovitch's finding that the PBC is not pertinent to a finite crystal in the presence of an electric field. We feel that this contradiction can (perhaps) be resolved by examining closely the translational symmetry related to the system and accounting properly for the surface levels to which the PBC gives rise in the presence of an electric field [Figs. 3, 4, 6(a), and 6(b) in our work].

B. Wave functions of the SL states

We note the following. *(a) Localization.* The wave functions of the SL states are found to be localized. This feature is also prevalent in the SL states in infinite systems, as was discussed by Wannier.[4(a)]

As mentioned in Sec. V, the localization of the wave functions of the SL states in finite systems was also studied by Saitoh[20]; he reported that for the occurrence of SL, the localization length ξ_l should satisfy the following condition:

$$\xi_l < L \, . \tag{6.1}$$

Condition (5.10) obtained by us is the analog of (6.1). For most practical cases, (5.10) would reduce to the following form:

$$\xi_l < 0.59L \, . \tag{6.2}$$

Looking at (6.1) and (6.2), we can say that, compared with Saitoh's finding, our investigation requires a sharper degree of localization of the wave functions for the occurrence of SL.

Worth discussing here are our results on the localization of the SL states with the numerical results of Nagai and Kondo,[26] in relation to the SL states in infinite systems. These authors studied numerically a one-dimensional infinite system with a Kronig-Penney potential. They found that Stark ladders occur in such infinite systems when the wave functions are localized, the criterion for a sharp localization of the wave functions being that Zener (interband) tunneling should be negligible. A close examination of Fig. 1 of Ref. 26 shows that the localization length for the SL states in the infinite system treated by Nagai and Kondo almost corresponds to our formula (5.7). Thus one can say that the localization of the wave functions characterizing the SL states is independent of the size of the crystal. However, our investigation has led additionally to the result expressed by inequality (6.2). This result, very significant for finite crystals, indicates that there may be localization of the wave functions and, yet, no Stark ladder may occur. What determines the occurrence of the Stark ladders is the condition that the degree of localization of the wave function should conform to the limit set by inequality (6.2).

(b) Translational symmetry of the wave functions. In Sec. V, we discussed how the wave functions of the SL states in a band exhibit translational symmetry [Eq. (5.6)]. The translational symmetry of the SL states was predicted by Wannier[4(a),4(b)] in connection with infinite crystals; our investigation shows that this feature is possessed by the SL states in finite crystals as well.

In conclusion, we would like to note that the periodic boundary condition is, as clearly discussed in the Introduction, the most physical boundary condition. The results obtained with the help of this boundary condition are, consequently, of considerable physical siginificance. It appears, however, that the quantitative study of the finite crystals in an electric field with the use of PBC has not yet received any attention. Viewed from these considerations, our exhaustive analyses of the energy spectrum and the wave functions with the application of the PBC are expected to resolve many (rather longstanding) controversies in regard to Stark ladders in finite systems.

ACKNOWLEDGMENTS

One of the authors (P.K.M.) would like to thank gratefully the Council of Scientific and Industrial Research (India) for a senior fellowship. The authors are also thankful to Professor G. B. Mitra for his interest and encouragement.

APPENDIX

As mentioned in Sec. IV, the purpose of this appendix is to discuss the mathematical features and the advantages relevant to Householder's tridiagonalization[29] method (HTD) and the *Q-L* algorithm[29]; these approaches were applied to (2.5) and (3.3) to determine the energy eigenvalues and the corresponding eigenvectors. The matrices $\underline{B}$ and $\underline{D}$, corresponding to (2.5) and (3.3), respectively, are real and symmetric; these properties being required because the matrices provide the energy eigenvalues ϵ, which are real. A symmetric matrix, say $\underline{B}$, can be brought to the diagonal form, $\underline{B}'$, as follows:

$$\underline{B}'=\underline{Z}^T\underline{B}\underline{Z}\,, \tag{A1}$$

where $\underline{Z}$ is an orthogonal matrix and $\underline{Z}^T$ is the transpose of $\underline{Z}$. The diagonal elements of $\underline{B}'$ are the eigenvalues of $\underline{B}$, and the kth column of $\underline{Z}$ contains the normed eigenvector corresponding to the kth eigenvalue of $\underline{B}$. The use of Householder's tridiagonalization method, in combination with the *Q-L* algorithm, is regarded[31] as the most efficient and the fastest procedure, when it is necessary to find out the complete set of eigenvalues and the eigenvectors pertinent to a symmetric matrix. These advantages lie substantially in the fact that the HTD method—the first phase of the approach towards diagonalizing a given symmetric matrix—brings, during every step of transformation, a complete row or a column to the desired form. This aspect of the HTD method has an edge over the other tridiagonalization methods[32] such as the Givens method; the latter kind of method, reduces to zero only one element at a time outside the three diagonals which alone are required to have nonvanishing elements. The HTD method thus requires fewer steps to reduce a given (symmetric) matrix to its tridiagonal form and becomes thereby relatively economical and accurate. The HTD method has another characteristic: the multiplication in every step can be carried out without round-off error; this characteristic adds considerably to the accuracy of the results. We outline below the mathematical aspects of the HTD method and then indicate the salient features of the *Q-L* algorithm, which performs the task of reducing to diagonal form the tridiagonal matrix obtained by the HTD method.

We consider the $M\times M$ matrix $\underline{B}$ which is symmetric and real. The HTD method reduces $\underline{B}$ to a tridiagonal form through $M-2$ similarity transformations, each of which brings an entire row and a column to the desired form. The matrices $\underline{P}^{(i)}$ which perform these similarity transformations are symmetric and involutary; explicitly, they appear as given below:

$$\underline{B}^{(i)}=\underline{P}^{(i)}\underline{B}^{(i+1)}\underline{P}^{(i)},\quad i=M,M-1,\ldots,3 \tag{A2}$$

$$\underline{P}^{(i)}=\underline{I}-\vec{U}^{(i)}[\vec{U}^{(i)}]^T/\Theta\,, \tag{A3}$$

$$\Theta=\tfrac{1}{2}[\vec{U}^{(i)}]^T\vec{U}^{(i)} \tag{A4}$$

is the normalizing factor,

$$\underline{B}^{(M+1)}=\underline{B}\,. \tag{A5}$$

$\vec{U}^{(i)}[\vec{U}^{(i)}]^T$ is a diadic product of a column vector $\vec{U}^{(i)}$ and its transposed (row) matrix $[\vec{U}(i)]^T$. The process starts with $i=M$, i being used as an index for the $M-2$ similarity transformations. For $i=M$, the elements of $\vec{U}^{(M)}$ appear as[30]

$$\begin{aligned}
&(U^{(M)})_M=0\,,\\
&(U^{(M)})_{M-1}=\frac{\sqrt{\Theta}[s\mp(B^{(M+1)})_{M,M-1}]^{1/2}}{\sqrt{s}}\,,\\
&(U^{(M)})_n=\mp\frac{(B^{(M+1)})_{M,n}\sqrt{\Theta}}{[s^2\mp s(B^{(M+1)})_{M,M-1}]^{1/2}}\,,
\end{aligned} \tag{A6}$$

where $n=1,2,\ldots,M-2$ and

$$s^2=\sum_{l=1}^{M-1}(B^{(M+1)})_{Ml}^2\,.$$

Using (A6) the elements of the transformed matrix $\underline{B}^{(M)}$ are obtained as

$$\begin{aligned}
(B^{(M)})_{pq}=(B^{(M+1)})_{pq}&-\frac{1}{v}(B^{(M+1)})_{Mq}\sum_{K=1}^{M-1}(B^{(M+1)})_{MK}(B^{(M+1)})_{Kp}-\frac{1}{v}(B^{(M+1)})_{Mp}\sum_{K=1}^{M-1}(B^{(M+1)})_{MK}(B^{(M+1)})_{Kq}\\
&+\frac{1}{v^2}(B^{(M+1)})_{Mp}(B^{(M+1)})_{Mq}\left[\sum_{K,R=1}^{M-1}(B^{(M+1)})_{MK}(B^{(M+1)})_{MR}(B^{(M+1)})_{RK}\right],
\end{aligned} \tag{A7}$$

where

$$v=[s^2\mp s(B^{(M+1)})_{M,M-1}].$$

In $\underline{B}^{(M)}$, the elements in the Mth row and column, except the diagonal and the (principal) subdiagonal elements, are zero. In the next step (i.e., $i=M-1$), the similarity transformation reduces the $(M-1)$th row and column to the proper form. When continued to $i=3$, the process gives the desired tridiagonal form of $\underline{B}$. The accumulated transformation matrix $\underline{Z}'$, relevant to this tridiagonalization, is given by

$$\underline{Z}'=(\underline{P}^{(M)}\underline{P}^{(M-1)}\cdots\underline{P}^{(3)}). \tag{A8}$$

We now consider the mathematical aspects related to the application of the Q-L algorithm. By applying this algorithm to the tridiagonal matrix resulting from the HTD method and the accumulated transformation matrix $\underline{Z}'$ concerned with it, we obtain the eigenvalues and the eigenvectors of the matrix $\underline{B}$. In the Q-L algorithm, similarity transformations are used for reducing the original tridiagonal matrix to a sequence of similar tridiagonal matrices, such that the off-diagonal elements become gradually smaller and smaller, and the tridiagonal matrix finally converges to the diagonal form.

The Q-L algorithm is defined as

$$\underline{B}^{(3)}_{s+1}=\underline{L}_s\underline{Q}_s^T, \tag{A9}$$

where

$$\underline{L}_s=\underline{Q}_s(\underline{B}_s^{(3)}-K_s\underline{I}), \tag{A10}$$

and $\underline{B}_1^{(3)}=\underline{B}^{(3)}$ is the tridiagonal matrix. $\underline{Q}_s$ is a unitary matrix and $\underline{L}_s$ is a lower triangular matrix; the term $K_s\underline{I}$ is introduced to improve the convergence of the nondiagonal elements to zero. $\underline{Q}_s$ can be determined in the factorized form

$$\underline{Q}_s=\underline{r}_1^{(s)}\underline{r}_2^{(s)}\cdots\underline{r}_{M-1}^{(s)}. \tag{A11}$$

The matrices $\underline{r}_n^{(s)}$ are determined in the order $\underline{r}_{M-1}^{(s)},\ldots,\underline{r}_1^{(s)}$; $\underline{r}_n^{(s)}$ is a rotation in the $(n,n+1)$ plane designed to annihilate the $(n,n+1)$th element. Before iterations for each eigenvalue, the symmetric tridiagonal matrix is checked for a possible splitting into submatrices. If a splitting occurs, only the uppermost submatrix participates in the next iteration, because the eigenvalues of each of the submatrices can be obtained without reference to the others. The iterations continue until the uppermost (1×1) principal submatrix splits from the rest of the matrix; its element is taken to be an eigenvalue and the algorithm proceeds with the remaining submatrix. The process continues until the matrix completely splits into submatrices of order 1, i.e., the matrix reduces to the diagonal form. The similarity transformation matrices $\underline{Q}_s^T$ are accumulated in $\underline{Z}$, which is defined as $\underline{Z}=\underline{Z}'\underline{Q}^T$; $\underline{Q}^T$ is the product of all the matrices $\underline{Q}_s^T$ connected with the Q-L algorithm. The kth column of $\underline{Z}$ represents the eigenvector corresponding to the kth eigenvalue of the matrix $\underline{B}$.

[1]F. Bloch, Z. Phys. 52, 555 (1928).
[2]C. Zener, Proc. R. Soc. London 145, 523 (1934).
[3]W. V. Houston, Phys. Rev. 57, 184 (1940).
[4](a) G. H. Wannier, Phys. Rev. 117, 432 (1960); (b) G. H. Wannier and D. R. Fredkin, *ibid.* 125, 1910 (1962); (c) G. H. Wannier, *ibid.* 181, 1364 (1969).
[5]J. Zak, Phys. Rev. Lett. 20, 1477 (1968); Phys. Rev. 181, 1366 (1969).
[6]C. A. Moyer, Phys. Rev. 87, 5025 (1973).
[7]J. E. Avron, Phys. Rev. Lett. 37, 1568 (1976).
[8]S. G. Davison and K. P. Tan, Z. Phys. 251, 6 (1972).
[9]S. G. Davison, Phys. Lett. 43A, 117 (1973).
[10]M. J. Richardson and S. G. Davison, Can. J. Phys. 52, 2395 (1974).
[11]J. Avron, L. Gunther, and J. Zak, Solid State Commun. 16, 189 (1975).
[12]T. Lukes and K. T. S. Somaratna, Phys. Lett. 29A, 69 (1969).
[13]C. L. Roy and P. K. Mahapatra, (a) Lett. Nuovo Cimento 24, 582 (1979); (b) 27, 117 (1980); (c) J. Phys. C 13, 5365 (1980).
[14]R. W. Koss and L. M. Lambert, Phys. Rev. B 5, 1479 (1973).
[15]J. Callaway, Phys. Rev. 134, A998 (1964).
[16]S. Maekawa, Phys. Rev. Lett. 24, 1175 (1970).
[17]M. Saitoh, J. Phys. C 5, 914 (1972).
[18]J. Heinrichs and R. O. Jones, J. Phys C 5, 2149 (1972).
[19](a) G. C. Stey and G. Gusman, J. Phys. C 6, 650 (1973); (b) C. L. Roy, Ind. J. Phys. 54, 5663 (1980).
[20]M. Saitoh, J. Phys. C 6, 3255 (1973).
[21]H. Fukuyama, R. A. Bari, and H. C. Fogedby, Phys. Rev. B 8, 5579 (1973).
[22]Vito Sessa and J. Sitte, J. Phys. C 11, 1599 (1978).
[23]J. R. Banavar and D. D. Coon, Phys. Rev. B 17, 3744 (1978).
[24]A. Rabinovitch and J. Zak, Phys. Rev. B 4, 2358 (1971).
[25]A. Rabinovitch, Phys. Lett. 59A, 475 (1977).

[26]S. Nagai and J. Kondo, J. Phys. Soc. Jpn. 49, 1255 (1980).
[27]A. Rabinovitch, Phys. Lett. 33A, 403 (1970).
[28]J. Villadsen and M. L. Michelsen, *Solution of Differential Equation Models by Polynomial Approximation,* edited by N. R. Amundson (Prentice-Hall, Englewood Cliffs, N.J., 1978).
[29]J. H. Wilkinson and C. Reinsch, *Handbook for Automatic Computation,* edited by F. L. Bauer *et al.* (Springer, Berlin, 1971), Vol. II.
[30]J. C. Slater, Phys. Rev. 87, 807 (1952).
[31]J. H. Wilkinson, *The Algebric Eigenvalue Problem,* edited by E. T. Goodwin and L. Fox (Oxford University Press, Oxford, 1965).
[32]H. R. Schwarz, H. Rutishausher, E. Steifel, and R. Hertendy, *Numerical Analysis of Symmetric Matrices,* edited by G. Forsythe (Prentice-Hall, Englewood Cliffs, N.J., 1973).